Influence of Monomer Structures on the High Temperature Properties of Poly[(Alkylamino)Borazine)]s Derived BN

Yongpeng Lei*, Yingde Wang and Yongcai Song

State Key Lab of Advanced Ceramic Fibers & Composites, College of Aerospace and Materials Engineering, National University of Defense Technology, Changsha 410073, P.R. China

Abstract: Preceramic polymers to boron nitride (BN) have been synthesized by thermal condensation of different (alkylamino)borazine monomers. Crystalline BN was obtained by pyrolysis of those polymeric precursors in NH_3 and then in Ar. The influence of monomer structure on the chemical composition, microstructure, oxidation resistance and high temperature stability of BN was investigated by a combination of elemental analysis (EA), density measurement, FTIR, XPS, XRD, HRTEM and TGA. With similar chemical composition, BN derived from symmetric monomer exhibited a higher crystallinity, better oxidation resistance and higher temperature stability. This was because that the structure of the precursor polymerized from symmetric molecular was close to that of hexagonal BN (*h*-BN).

Keywords: Molecular structure, polymer-derived ceramics, microstructure, high temperature properties.

1. INTRODUCTION

Due to its high melting point, good thermal conductivity, high temperature stability and superior oxidation resistance, boron nitride (BN) has been a potential non-oxide ceramic material for aircraft and space applications [1, 2]. The most promising approach for the fabrication of shaped BN such as fiber, film, and mesoporous material is polymer-derived ceramics (PDCs) method [3-6]. Alkylaminoborazines (AAB) derived from 2,4,6-trichloroborazine (TCB) have been deemed to be attractive molecular monomers for processable polymers to BN in a complex form [7-9]. Nonetheless, as far as we know, it was not easy to synthesize AAB monomers to processable polymers due to the measurement of gaseous alkylamines [10].

Our attention has been focused on the synthesis of various monomers to melt-spinnable precursors using appropriate alkylamines and TCB without extraordinarily low temperature [7, 11]. The reactivity of AAB monomers, which were in close connection with the processability of polymeric precursors, was strongly dependent on the substituent alkylamino groups linked with boron atoms [7, 10, 12]. However, the research that the structural influence of monomer on the poly[(alkylamino)borazine)]s derived BN's high temperature properties was limited, except that Toury *et al*. compared the crystallinity of BN from different molecular precursors [13]. Considering BN's excellent potential in structural/functional applications, it is necessary to investigate the high temperature properties of BN derived from various molecular monomers [14].

In this work, preceramic polymers were synthesized by thermal condensation of different (alkylamino)borazine monomers as reported by our own lab earlier [7, 11]. By pyrolysis of the polymeric precursors under the same condition, nearly stoichiometric BN with similar composition but different microstructure and crystallinity were obtained. Oxidation behavior and high temperature stability of two BN sample were investigated. The difference in high temperature properties depends significantly on the crystallinity of BN originated from different (alkylamino)borazine monomers.

2. EXPERIMENTAL

All experiments were carried out in a nitrogen atmosphere using standard vacuum-line, Schlenk techniques and an efficient dry box with solvents purified by standard methods [15]. TGA was performed on a NETZSCH STA 449C instrument in Ar or air at a heating rate of 10 °C/min. Boron content was measured by a chemical titration method. Element contents of N, O, H and C were checked by Leco TCH-600 N/H/O and Leco CS-600 C/S analyzers. FTIR spectra were collected on a Nicolet Avatar 360 spectrophotometer as KBr pellets. XRD patterns were recorded using a powder X-ray diffractometer (Siemens D-5005, Cu K_α radiation). The average grain size was estimated by the Scherrer equation [16]. The XPS spectra were obtained using a VG ESCALAB MKII instrument (Al K_α excitation). Density was measured by floatation in halogenated hydrocarbons. The HRTEM image was taken with a Philips CM 200 transmission electron microscope operated at 200 kV.

Molecular monomers TAB and PAB were synthesized by aminolysis reactions of 2,4,6-trichloroborazine (TCB) with *iso*-propylamine and *n*-propylamine/methylamine, respectively. PTAB and PPAB were prepared by thermal condensation of TAB and PAB described in our earlier work [7, 11]. The molecular structures of monomers and polymers were shown in Table **1**.

PTAB: FTIR (KBr/cm^{-1}): 3421/3134/1031 cm^{-1} (N-H), 2924/2853 cm^{-1} (C-H), 1400 cm^{-1} (B-N), 745 cm^{-1} (B-N-B), 1078 cm^{-1} (C-N). ^{13}C-NMR (ppm): δ 8.9 (-CH_3), 25.9 (-

*Address correspondence to this author at the State Key Lab of Advanced Ceramic Fibers & Composites, College of Aerospace & Materials Engineering, National University of Defense Technology, Changsha 410073, China; Tel/Fax: +86 731 84575118; E-mail: lypkd@yahoo.com.cn

1874-088X/12

CH_2CH_3), 45.9 (-$NHCH_2$), 55.1 (-NCH_2). Elemental analysis (wt%): B 23.13, C 22.67, N 44.70, O 0.97, H 8.33.

Table 1. Molecular Structure of the Monomers and Preceramic Polymers

	Name	Chemical Structure
Monomer	TAB	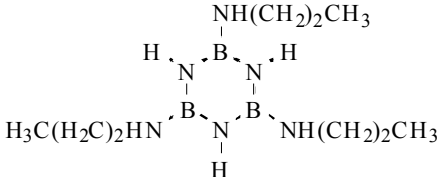
	PAB	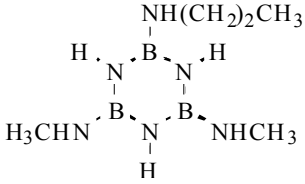
Polymer	PTAB	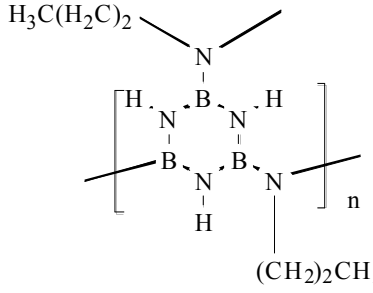
	PPAB	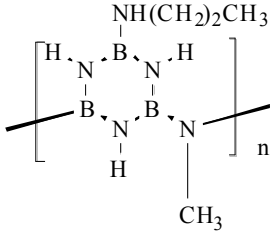

PPAB: FTIR (KBr/cm^{-1}): 3414/3130/1021 cm^{-1} (N-H), 2962 cm^{-1} (C-H), 1400 cm^{-1} (B-N), 805 cm^{-1} (B-N-B), 1092 cm^{-1} (C-N). ^{13}C-NMR (ppm): δ 19.3 (-CH_3), 43.4 (-NHCH), 50.3 (-NCH-). Elemental analysis (wt%): B 25.12, C 18.79, N 45.16, O 0.82, H 8.04.

In a typical pyrolysis procedure, the polymer precursor lumps were milled using a tungsten carbide ball mill and sieved into particles in the size < 32 μm. Then the powders were weighed into an alumina boat and then placed in the pyrolysis tube. After purging the system with Ar for 30 min, the samples were heated at 4 °C/min to 1000 °C in NH_3 (60 ml/min) with a holding time of 2 h before cooling to ambient temperature naturally. Subsequently, the pyrolysis products were annealed under flowing Ar at 1500 °C in a graphite furnace with a holding time of 1 h (heating rate, 5 °C/min).

3. RESULTS AND DISCUSSION

Fig. (**1**) displays the FTIR spectra of pyrolyzed samples from PTAB and PPAB at 1500 °C (called BN_{PTAB} and BN_{PPAB}), which were almost the same. The very intense absorption at 1394 cm^{-1} and weak absorption at 804 cm^{-1} can be assigned to the ν (B-N) and δ (B-N-B), respectively [17]. Moreover, the N-H band located around 3400 cm^{-1} indicated the presence of little residual hydrogen in the pyrolyzed samples.

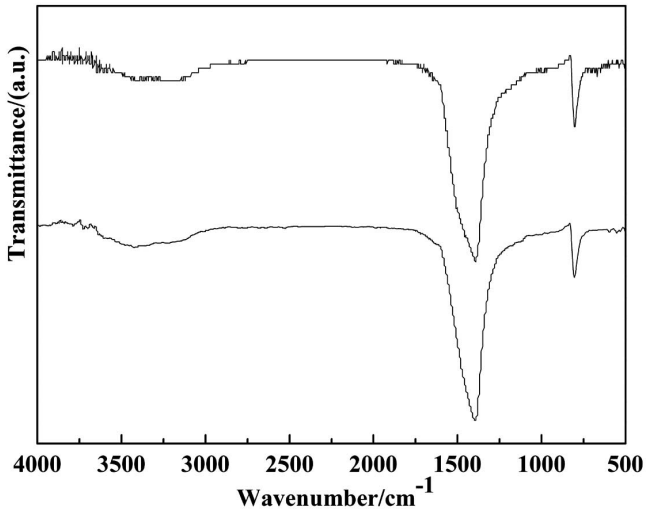

Fig. (1). FTIR spectra of pyrolyzed samples derived from (**a**) PTAB and (**b**) PPAB.

The chemical composition of the pyrolyzed products was investigated. The B/N ratios of BN_{PTAB} and BN_{PPAB} at 1500 °C were 1:1.07 and 1:1.05 determined by EA, respectively. And carbon contents were both less than 0.2 wt%, demonstrating the successful removal of carbon and preparation of nearly stoichiometric BN from alkylamino-containing precursor. The densities for two BN samples were also similar, 1.81 g·cm^{-3} (BN_{PPAB}) and 1.85 g·cm^{-3} (BN_{PPAB}), respectively.

In order to further identify chemical bonding of the pyrolyzed products, XPS were conducted on two pyrolyzed products. The wide-scan XPS spectra of BN_{PTAB} (Fig. **2a**) indicated the presence of B, N, C and O element. The C1s signal may arise from different contamination. The presence of O element was mainly due to the absorption of oxygen species in form of O_2 and CO_2. The split B1s and N1s spectra of BN_{PTAB} were shown in Fig. (**2b**, **c**). The B1s peak at 190.8 eV and the N1s peak at 397.7 eV indicated BN, consistent with the previous reports on BN [18]. The XPS spectra of BN_{PPAB} (not illustrated) were similar to that of BN_{PTAB}.

The Raman spectra of two pyrolyzed products were shown in Fig. (**3**). In Fig. (**3a**), the spectrum was typical of *h*-BN with a signal at 1374 cm^{-1}. While in Fig. (**3b**), the large width of the band around 1500 cm^{-1} represented a noncrystalline BN [19]. The full width at half maximum (FWHM) was also much broader than that in BN_{PTAB}, indicating a lower crystallinity of the BN phase existed in BN_{PPAB} [20]. The difference in crystallinity would be confirmed later on.

The crystalline structure of the BN phase was examined by XRD, as seen in Fig. (**4**). The FWHM of the (002) peak in BN_{PTAB} was narrower than that in BN_{PPAB}, indicating a higher crystallinity and larger grain size. The peaks at 2θ=41.6º, 43.5º, 82.1º in BN_{PTAB} were ascribed to the (100), (110) and (112) planes, respectively. But yet (100) and (101)

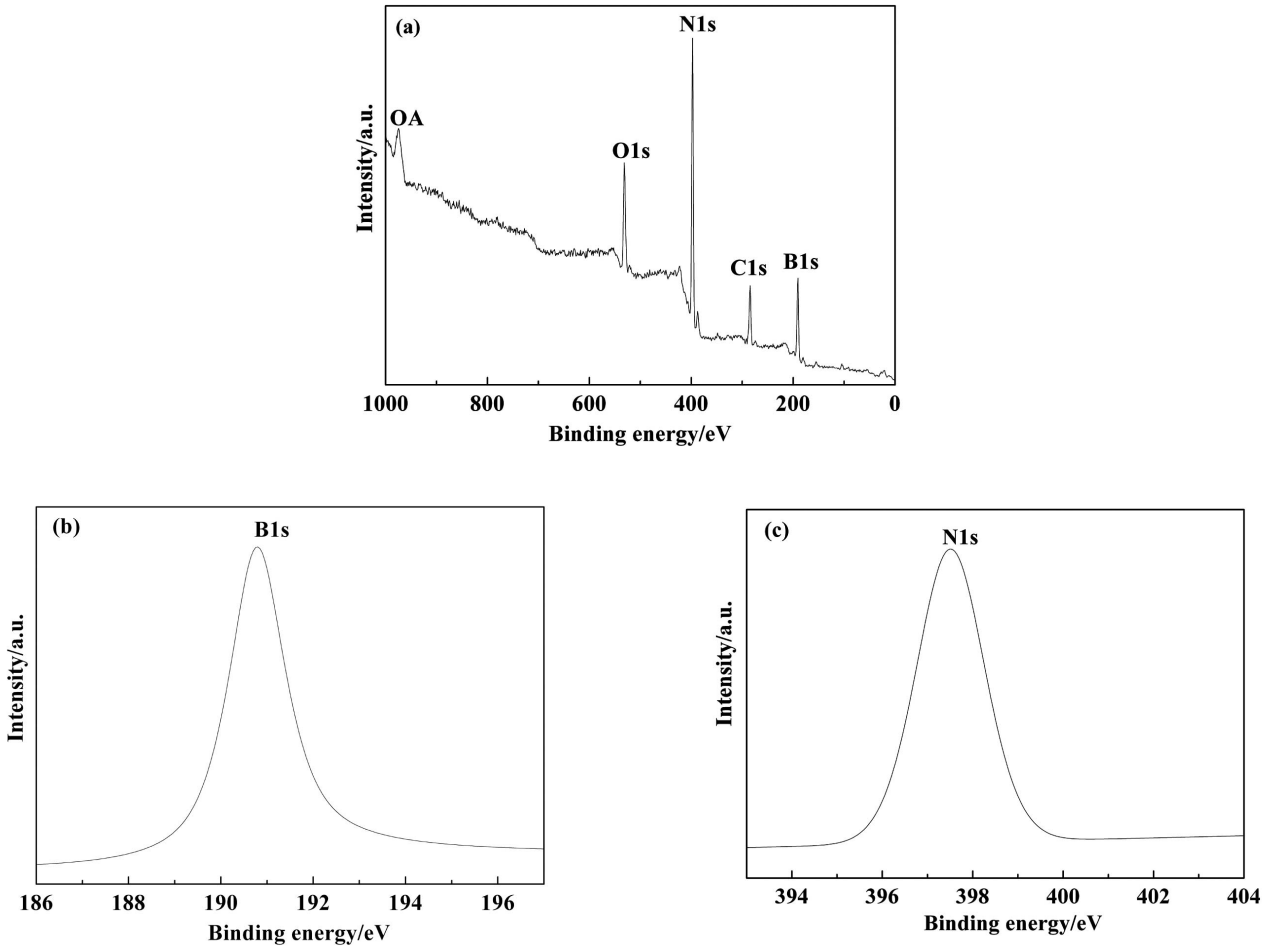

Fig. (2). XPS spectra of BN_{PTAB} (**a**) wide-scan, (**b**) B1s and (**c**) N1s.

reflections in BN_{PPAB} were indissociable and (112) was absent, suggesting the turbostratic character. Furthermore, the difference in the XRD patterns of those products further annealing at 1800 °C was more obvious. The samples annealing at 1800 °C derived from PTAB displayed a sharp (002) plane and other planes changed more evident compared to those obtained at 1500 °C. While the XRD patterns of the residue from PTAB at 1800 °C changed little.

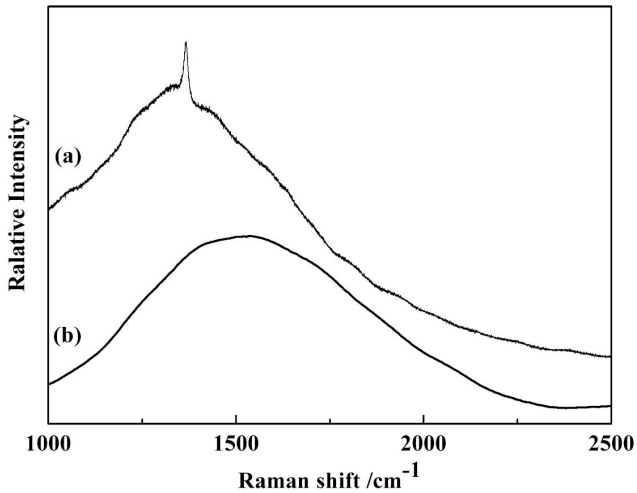

Fig. (3). Raman spectra of (**a**) BN_{PTAB} and (**b**) BN_{PPAB}.

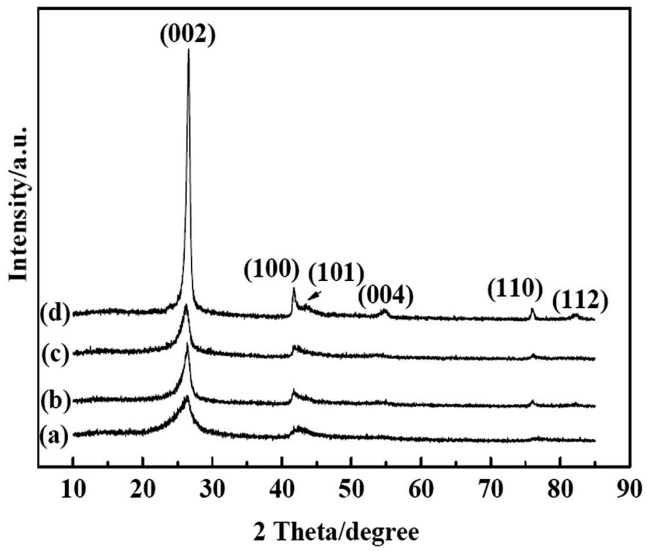

Fig. (4). XRD patterns of: (**a**, **b**) BN_{PPAB} and BN_{PTAB} obtained at 1500 °C, (**c**, **d**) BN_{PPAB} and BN_{PTAB} at 1800 °C.

In addition, the average interlayer spacing (d_{002}) and grain size (L_{002}) were 3.36 Å/7.542 nm (BN_{PTAB}) and 3.40 Å/5.320 nm (BN_{PPAB}) evaluated from the (002) diffraction, respectively. The results give a hint that symmetric molecular derived BN had a higher crystallinity over asymmetric molecular derived. Polymeric precursor whose

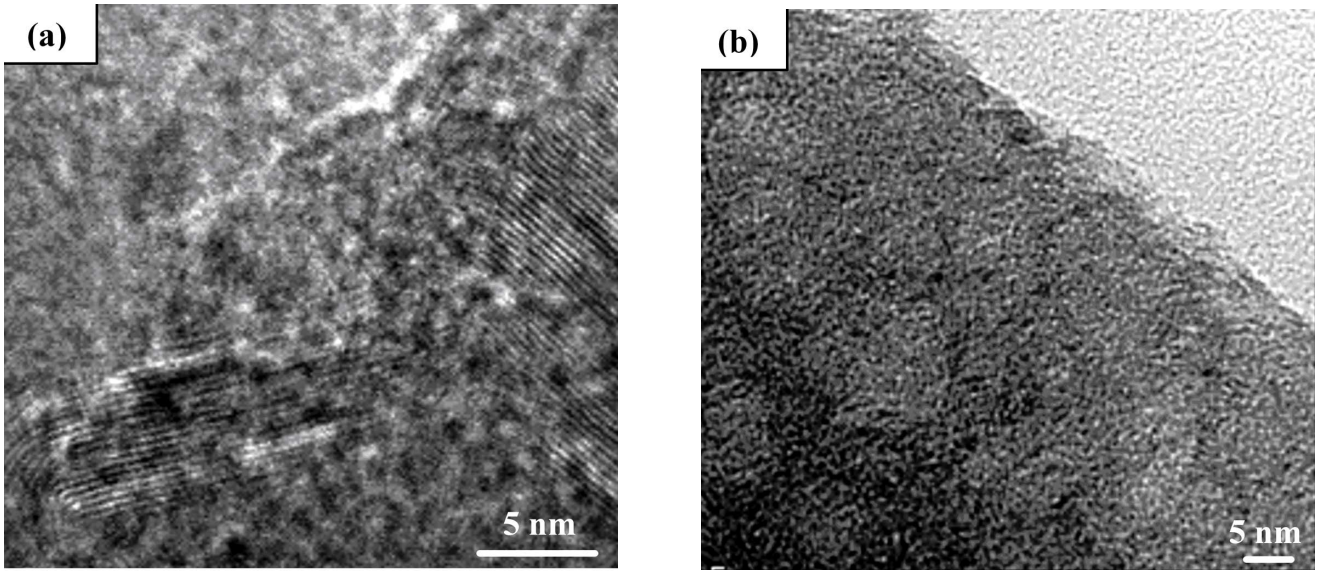

Fig. (5). HRTEM images of (**a**) BN_{PTAB} and (**b**) BN_{PPAB}.

structure was closer to that of *h*-BN gave more-crystallized BN, as Toury *et al.* studied [13]. PPAB was composed of B_3N_3 rings most bonded through -B-N(CH_3)-B- bridges. But yet, B_3N_3 rings in PTAB were linked with more -B-N- bridges and little -B-N[$CH_3(CH_2)_2$]-B- bridges, much closer to the structure of *h*-BN.

Further detailed investigation on the BN's microstructure was researched by HRTEM, as shown in Fig. (**5**). An important difference was noticed due to different crystallinity. In Fig. (**5a**), partially crystallized BN in some locally inhomogeneous regions was observed. While in Fig. (**5b**), a homogeneous amorphous phase was noticed [21]. This conclusion agrees well with that obtained from the XRD patterns.

Subsequently, the oxidation behaviors of two samples were studied under a flow of air at temperature up to 1000 °C, as shown in Fig. (**6**). It is clear that BN_{PTAB} showed an excellent stability with only a small detectable weight loss of 1.2 wt% at 900 °C. In comparison, BN_{PPAB} began to lose weight at around 270 °C and displayed a weight loss of 2.5 wt% at 900 °C. Furthermore, onset oxidation temperature for BN_{PTAB} was a little higher than that for BN_{PPAB}. For two samples, the weight loss below 900 °C may be due to vaporization of B_2O_3 formed on the original surface of BN under normal room temperature [22]. Besides, BN_{PTAB} showed a slower weight increase than BN_{PTAB} above 900° C. The weight increase was due to the formation of B_2O_3 according to eq.(1) and eq.(2) below. The discrepancy in oxidation rate between two BN samples was caused by different crystallinity that BN with a lower crystallinity showed a lower oxidation rate [23].

To investigate the high temperature stability of the as-prepared BN, the TGA experiment was carried out at temperature up to 1300 °C under flowing Ar. Fig. (**7**) displays the TGA curves of two samples. As expected, both BN presented good high-temperature stability up to 1300 °C. A final weight loss of 1.4 wt% and 4.1 wt% were observed for BN_{PTAB} and BN_{PPAB}, respectively, indicating a higher stability of BN_{PTAB}. The weight loss may also result from vaporization of B_2O_3, as discussed above.

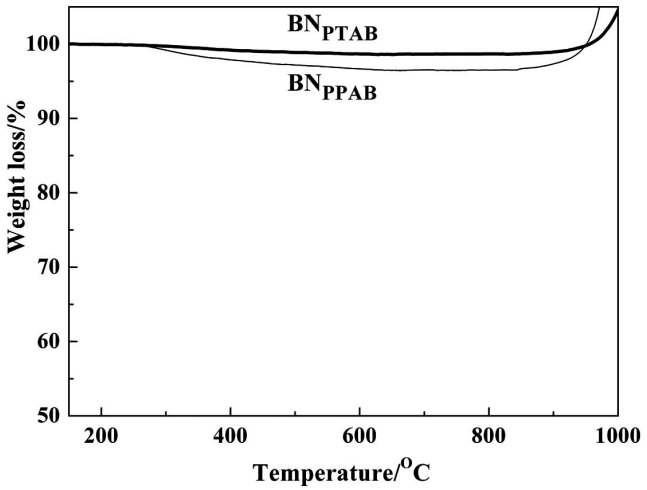

Fig. (6). TGA curves of BN_{PTAB} and BN_{PPAB} in flowing air.

$$4BN\ (s)+3O_2\ (g)\rightarrow B_2O_3\ (l)+2N_2\ (g) \quad (1)$$

$$2BN\ (s)+3H_2O\ (g)\rightarrow B_2O_3\ (l)+3H_2\ (g)+N_2\ (g) \quad (2)$$

4. CONCLUSIONS

Two poly[(alkylamino)borazine]s were obtained by thermal condensation of different molecular monomers. By pyrolysis of two polymers separately, nearly stoichiometric BN samples without carbonaceous impurities were acquired. The chemical composition of both BN was similar, while the crystallinity and microstructure were different. It seems that the symmetric molecular structure gave BN a higher crystallinity and better oxidation resistance /high temperature stability. The present work provides a better understanding that the influence of the molecular monomer structure on high temperature properties of polymer-derived BN.

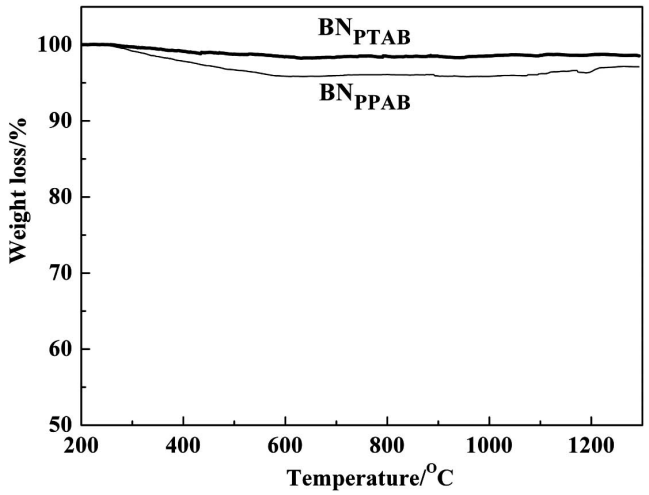

Fig. (7). TGA curves of BN_{PTAB} and BN_{PPAB} in flowing Ar.

ACKNOWLEDGEMENT

The work was financially supported by National High technology Research and Development of China (No. 2006AA03A217).

CONFLICTS OF INTEREST

Declared none.

REFERENCES

[1] Paine RT, Narula CK. Synthetic routes to boron nitride. Chem Rev 1990; 90: 73-91.

[2] Li S, Bernard S, Salles V, Gervais C, Miele P. Preparation of polyborazylene-derived bulk BN with tunable properties by warm-pressing. Chem Mater 2010; 22: 2010-7.

[3] Miele P, Bernard S, Cornu D, Tourya B. Recent developments in polymer-derived ceramic fibers (PDCFs): preparation, properties and applications - a review. Soft Mater 2007; 4: 249-86.

[4] Chu ZY, Feng CX, Song YC, Li XD, Xiao JY. Synthesis of polyborosilazane and its utilization as a precursor to boron nitride. J Appl Polym Sci 2004 ; 94 : 105-9.

[5] Tang Y, Wang J, Li XD, *et al*. Polymer-derived SiBN fiber for high-temperature structural/functional applications. Chemistry 2010; 16(22): 6458-62.

[6] Tang Y, Wang J, Li XD, *et al*. One-pot synthesis of novel polyborosilazane to SiBNC fibres. Inorg Chem Comm 2009; 12: 602-4.

[7] Deng C, Song YC, Wang YD, Li YH, Lei YP. Preparation and characterization of polymeric precursor for boron nitride fibers. Chem Res Chin Univ 2010; 31: 623-8. (In Chinese).

[8] Toury B, Bernard S, Cornu D, *et al*. High-performance boron nitride fibers obtained from asymmetric alkylaminoborazine. J Mater Chem 2003; 13: 274-9.

[9] Lei YP, Wang YD, Song YC, *et al*. Nearly stoichiometric BN fiber with low dielectric constant derived from poly[(alkylamino)borazine]. Mater Lett 2011; 65: 157-9.

[10] Toury B, Miele P, Cornu D, Vincent H, Bouix J. Boron nitride fibers prepared from asymmetric and asymmetric alkylaminoborazines. Adv Funct Mater 2002; 12: 228-34.

[11] Lei YP, Wang YD, Song YC, *et al*. Facile synthesis of a melt-spinnable polyborazine from asymmetric alkylaminoborazine. Chin Chem Lett 2010; 21: 1079-82.

[12] Deng C, Song YC, Wang YD, *et al*. Synthesis of polymeric precursor for boron nitride through substitution reaction of methyalmine/dimethylamine. Acta Chim Sinica 2010; 68: 1217-22. (In Chinese).

[13] Toury B, Duriez C, Cornu D, *et al*. Influence of molecular precursor structure on the crystallinity of boron nitride. J Solid State Chem 2000; 154: 137-40.

[14] Lei YP, Wang YD, Song YC, *et al*. Effect of molecular monomer structure on the composition and properties of BN *via* the preceramic polymer route. Mater Lett 2011; 65: 1111-3.

[15] Perrin DD, Armarego WL, Perrin DR. Purification of laboratory chemicals. London: Pergamon Press 1966.

[16] Jenkins R, Snyder RL. Introduction to X-ray powder diffractometry. New York: Wiley Press 1996.

[17] Xu LQ, Peng YY, Meng ZY, *et al*. A co-pyrolysis method to boron nitride nanotubes at relative low temperature. Chem Mater 2003; 15: 2675-80.

[18] Jeon JK, Uchimaru Y, Kim DP. Synthesis of novel amorphous boron carbonitride ceramics from the borazine derivative copolymer *via* hydroboration. Inorg Chem 2004; 43: 4796-8.

[19] Rye RR, Tallant DR, Borek TT, Lindquist DA, Paine RT. Mechanistic studies of the conversion of borazine polymers to boron nitride. Chem Mater 1991; 65: 286-93.

[20] Termoss H, Toury B, Pavan S, *et al*. Preparation of boron nitride-based coatings on metallic substrates *via* infrared irradiation of dip-coated polyborazylene. J Mater Chem 2009; 19: 2671-4.

[21] Termoss H, Toury B, Brioude A, *et al*. High purity boron nitride thin films prepared by the PDCs route. Surf Coat Technol 2007; 201: 7822-8.

[22] Yang ZH, Jia DC, Zhou Y, *et al*. Oxidation resistance of hot-pressed SiC-BN composites. Ceram Int 2008; 34: 317-21.

[23] Cofer CG, Economy J. Oxidation and hydrolytic stability of boron nitride - a new approach to improving the oxidation resistance of carbonaceous structures. Carbon 1995; 33: 389-95.

Received: December 12, 2011 Revised: February 21, 2012 Accepted: February 22, 2012